The CoRoT Legacy Book

DOI: 10.1051/978-2-7598-1876-1.c043

IV.3
The wealth of stellar variability
Stellar rotation and activity, Binaries and Stars with disks

F. Baudin[1], C. Maceroni[2], and S. H. P. Alencar[3]

[1] Institut d'Astrophysique Spatiale, UMR8617, CNRS, Université Paris XI, Bâtiment 121, 91405 Orsay Cedex, France
[2] INAF-Osservatorio Astronomico di Roma, via di Frascati 33, 00040 Monteporzio Catone, Italy
[3] Departamento de Física – ICEx – Universidade Federal de Minas Gerais Av. Antônio Carlos, 6627 – 31270-901 Belo Horizonte, MG – Brasil

1. Introduction

CoRoT made a decisive step forward not only in stellar seismology and galactic populations studies but also in a number of other physical phenomena encompassed by stellar variability. Surface activity is one example and is the outward sign of surface rotation and magnetic activity as described in Sect. 2. In this domain, CoRoT observations motivated the investigation of the surface rotational behavior of stars along with their evolution (Sect. 2.1), the highlighting of spot evolution and magnetic cycles (Sect. 2.2), as well as the study of surface convection across the Hertzsprung–Russell diagram (Sect. 2.3). CoRoT's dataset then opened the way to a multivariate-like approach in which rotation, convection, and magnetic field are investigated together as key ingredients of stellar dynamos. Moreover, it is worth mentioning that such studies were previously restricted to the Sun but, with the advent of ultra-precise and long-duration photometry, we are beginning to address similar issues in other stars.

CoRoT also led to important advances in the field of binary stars as described in Sect. 3. Indeed, a few targets in the bright fields were dedicated to the observation of known binaries but it appears that a large number of binaries have been discovered in the faint fields. As for red giants, this led to a number of discoveries and surprises. For instance, it allowed for statistical investigations (Sect. 3.1) as well as the discovery of new type of binary stars (Sect. 3.2). In that respect, CoRoT's main contributions relied on the precision and the duration of the observations which made it possible to follow the evolution of several binary systems and to unravel physical processes occuring on different time-scales. Finally, CoRoT's observations demonstrated the fruitful synergy between binarity and asteroseismology as a tool for determining independently the stellar parameters of each component (Sect. 3.3).

Last but not least, a rich harvest of observational constraints has been obtained on young stars as described in Sect. 4. This allowed a further step in our knowledge of star-disk interactions which is crucial for the scenarios of star formation but also for our understanding of the initial steps of stellar evolution. A striking example is the coordinated synoptic investigation of NGC 2264 (Sect. 4.2), which consisted in a multiwavelenght observational campaign including space-borne and ground-based facilities. Due to its intrinsic abilities, CoRoT contributed significantly by providing 40 days of continuous observations. This campaign made it possible to investigate several young stars and their environement by providing a wealth of data which led to a harvest of scientific results.

2. Stellar rotation and activity (by F. Baudin)

The two main objectives of the CoRoT mission (namely search for exoplanets and stellar seismology) were based on a sole capacity: ultra precise photometry. This capacity allows many more scientific objectives to be aimed at, concerning the physics responsible for the micro-variability of stars, beyond that caused by oscillations. Manifestations of magnetic fields and signature of granulation are among the main sources of this micro-variability (binaries or stellar disks for example are others, see Sects. 3 and 4).

2.1. Thousands of star's rotation periods measured

Stars show very different behaviors concerning their rotation. Some rotate faster than others, some show differential rotation (in surface or in their interior - but here, we will focus on surface rotation). These behaviors are related to the structure and evolution of the stars and are also a fondamental ingredient of stellar magnetism (with a direct application to gyrochronology). Rotation is driven by several

mechanisms, mainly star contraction and expansion during its evolution, but also its interaction with its disk in its early phases of evolution. CoRoT data, thanks to their ultra-high photometric precision for a very large sample of stars, are perfectly suited to tackle the questions related to these physical mechanisms.

Among works aiming at rotation measurements based on CoRoT data, Affer et al. (2012) used some of the first observation runs, LRc01 and LRa01, thus covering field stars in the center and anti-center directions. An initial sample of 8341 light curves was used to measure rotation periods by two methods: the Lomb-Scargle Normalized periodogram and an auto-correlation analysis. About 2000 light curves had to be rejected because of the discontinuities caused by particle impacts on the detector[1]. Finally, after checking for coherence between the two analysis methods and some other rejections (due for example to eclipsing binaries or pulsators), a total of 1727 periods of rotations were reliably measured, including F, G and K stars (however, only 4 F stars were identified in the center direction preventing any interpretation). Resulting distributions show bimodal shapes (Fig. IV.3.1). A first peak, with periods from 5 to 15 days is interpreted as representing a population of young stars, while a second peak, including periods from 15 to 35 days is interpreted as due to an older population. Using gyrochronology expressing the rotation period as a function of age and $B-V$, Affer et al. (2012) have found that more than 500 stars of their sample are younger than the Hyades (∼650 Myr). The observed sample is consistent with results from X-ray surveys supporting the presence of an excess of young stars in the solar neighborhood. However, as pointed out by the authors, it should not be forgotten that the CoRoT sample is biased towards dwarfs because of the exoplanet search objective that drove the target selection.

An even larger analysis was performed by De Medeiros et al. (2013) who started from all light curves available at that time (a total of 124 471). The analysis was based on a semi-automated process and a severe selection of light curves in order to ensure the reliability of the results. Among other criteria, this selection process rejected low signal-to-noise ratios and tested against signals that could mimic that of rotation modulation, such as semi-regular pulsators'. Attention was also paid to the influence of discontinuities in the data[1]. This process resulted in the measurement of 4206 rotation periods, across the H-R diagram (Fig. IV.3.3). 216 targets were common with Affer et al. (2012) and the results show an excellent agreement with them. Results (Fig. IV.3.4) show an increase of rotation periods with the color difference $J-H$ (which increases with increasing effective temperature - for main sequence stars and unreddened measurements). This increase can be at least partially explained by evolution since higher values of $J-H$ correspond to a bias towards evolved –thus rotating slower– stars, as seen in Fig. IV.3.3 . An excess of long periods is noted in the galactic center, due to an excess of giants, whereas in the total sample, only one star is similar to the Sun in terms of rotation period and $J-H$ value.

As mentioned by several authors, rotation measurements are obviously biased towards young stars since they are more active and thus showing clearer photometric

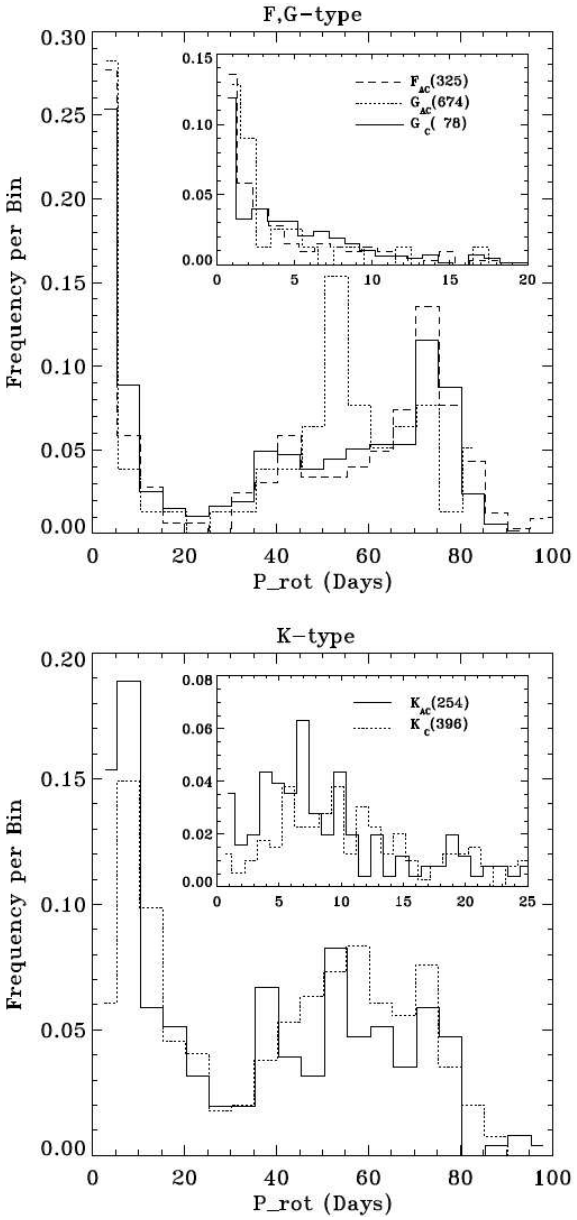

Fig. IV.3.1. Figure 10 of showing the bi-modal distribution of the rotation periods of the field stars they studied © MNRAS, 424, 11.

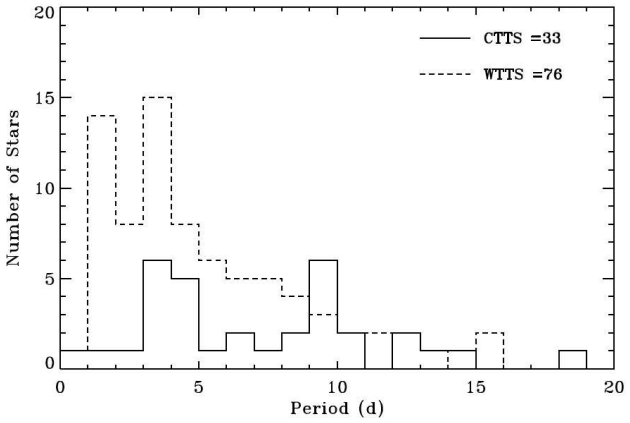

Fig. IV.3.2. Figure 5 of showing the distribution of the rotation periods of the CTTS and WTTS stars they studied © MNRAS, 430, 1433.

[1] Early versions of data were used for this work but most of these discontinuities are now corrected in the final version.

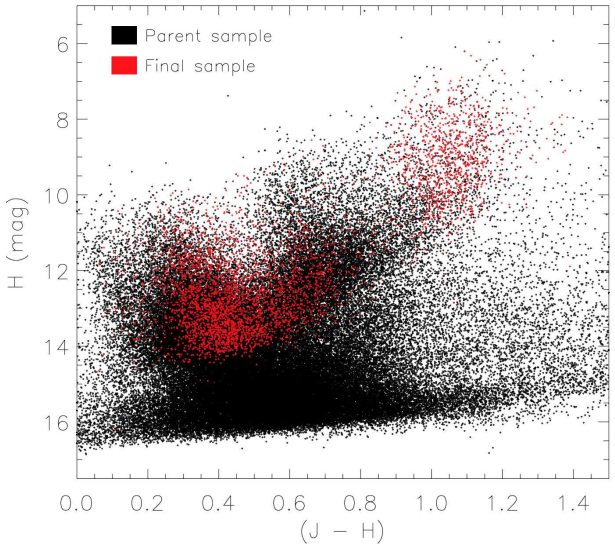

Fig. IV.3.3. Figure 9 of De Medeiros et al. (2013), showing the total number of targets considered at the start (in black) and the remaining ones at the end of the process (see text) © A&A.

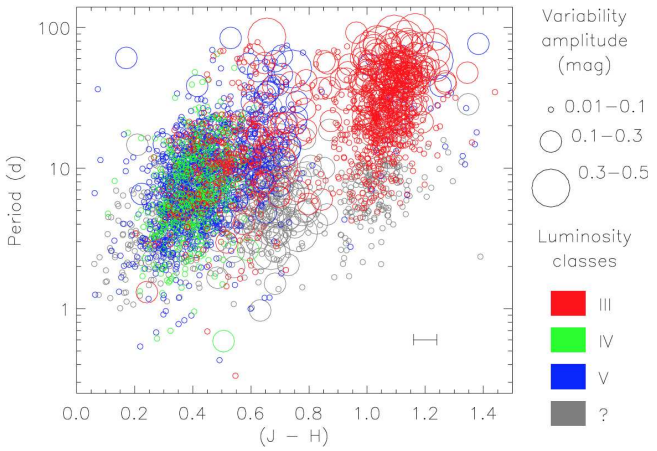

Fig. IV.3.4. Figure 13 of De Medeiros et al. (2013), showing the rotation periods measured versus the color index $J - H$. Symbol size relates to variability amplitude and color to luminosity class. The increase seen is compatible with stellar evolution © A&A.

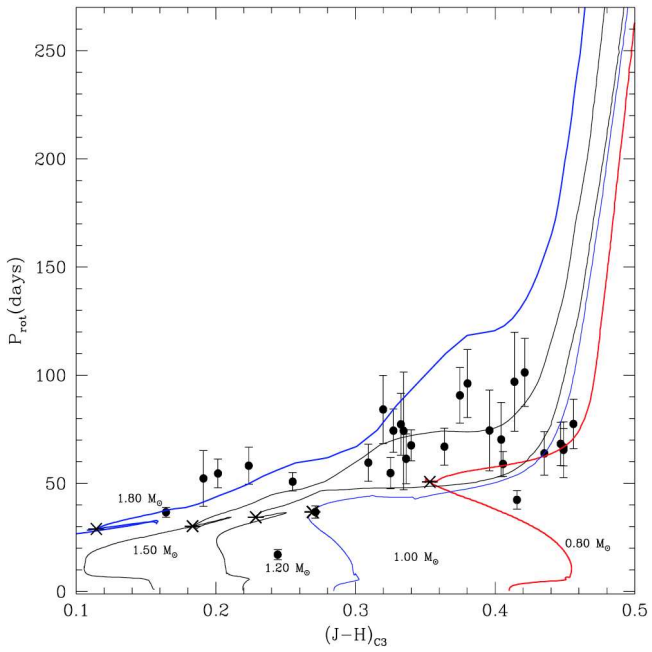

Fig. IV.3.5. Figure 3 of do Nascimento et al. (2012), showing the periods measured (black filled circles) and evolution tracks versus the color difference. $(J - H)_{C_3}$ relates to a combination of colors minimizing the effect of reddening. Asterisks locate the beginning of the sub giant branch © A&A.

modulation due to rotation. Stars similar to the Sun in terms of mass and age, with periods around solar values are thus rare. One case was found by do Nascimento et al. (2013) after a detailed analysis of CoRoT targets (using spectroscopic results from Sarro et al. 2013): CoRoT-102684698 which has a similar mass and also similar Lithium abundance, and a period $P_{\rm rot} = 29 \pm 5$ days.

However, any conclusion about stars sharing solar characteristics is made very difficult due to their very small number. In order to estimate if the Sun's rotation is anomalous or not, Leão et al. (2015) deepen the work of De Medeiros et al. (2013) by selecting a subsample from their catalog (plus other samples from *Kepler* catalogs), gathering solar type stars and comparing them to synthetic samples built in order to take into account the low number of solar rotators. Leão et al. (2015) propose that their subsample of 173 stars with $T_{\rm eff}$ and $\log(g)$ close to solar values is made of two populations, one of young stars, more numerous than the other group made of older stars. From global results based on CoRoT and *Kepler* data, they do not evidence an anomalous rotation period for the Sun.

More focused rotation period measurements were also performed. Affer et al. (2013) applied the same method than Affer et al. (2012) to T Tauri stars observed in NGC2264, a young cluster (3 Myr) in the solar vicinity (760 pc) observed for ∼23 days during run SRc01. Two well separated sub-categories of stars were selected: the Weakly T Tauri Stars (WTTS, for which variaability is induced by spots) and Classical T Tauri Stars (CTTS, for which variability is due to the presence of a disk). Rotation was measured for 76 WTTS and 33 CTTS. Despite the small size of the samples, a clear difference is seen (Fig. IV.3.2): CTTS are slower rotators (with a mean rotation period $\langle P_{\rm rot} \rangle = 7.0$ days) than WTTS ($\langle P_{\rm rot} \rangle = 4.2$ days). This is interpreted as the result of the presence of an inner disk for CTTS, slowed down by disk locking due to strong magnetic fields. This in turn can help in constraining the interactions between the star and its disk that will drive the rotation history of a young star.

Another focused work is the one of do Nascimento et al. (2012) who measured the rotation periods of subgiants, analyzing only long duration light curves (150 days). This allowed the measurement of slow rotators, with $P_{\rm rot}$ between 30 and 100 days. These periods are in good agreement with the modeling of stellar evolution including rotation of the Fig. IV.3.5, validating the description of late rotation evolution for stars of the masses considered here.

2.2. Stellar magnetic activity measured down to the spot level

Since one of the main scientific objective of CoRoT is the detection of transiting planets in front of their parent star,

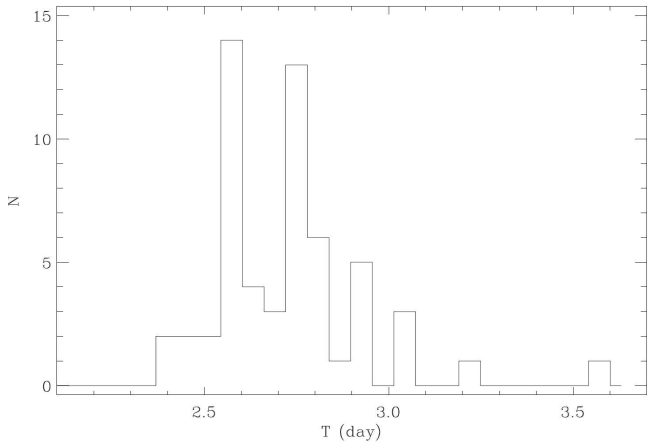

Fig. IV.3.6. Figure 6 of Mosser et al. (2009a), showing the distribution of rotation periods of individual spots. Their distribution is consistent with the wide rotation peak observed in the Fourier spectra of the light curve © A&A.

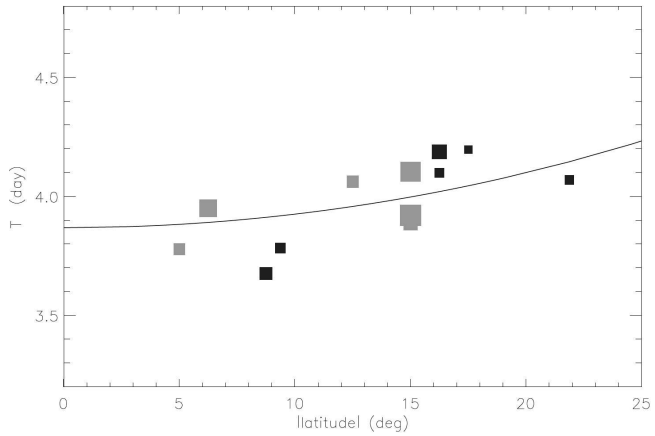

Fig. IV.3.7. Figure 8 of Mosser et al. (2009a), showing the rotation period of individual spots increasing with their latitude, as a signature of differential rotation © A&A.

its ultra-high photometric precision allows also the detection of transiting inhomogeneities on stellar surfaces. The most visible are magnetic spots, like sunspots which signature is visible in disk-integrated solar light curves. The clear signature of starspots in some CoRoT light curves allows the modeling of the observed intensity variation by assuming simple models of starspots. An extreme example is HD175726, showing intensity peak-to-peak variations up to 1% (Mosser et al. 2009b).The difficulty lies in the degeneracy of the problem since many parameters are necessary to describe the signature of a transiting starspot: its size and intensity contrast (obviously correlated), its intrinsic temporal behavior (which is modulated by the rotation period) but also its position on the star (linked to the inclination angle of the star). Several methods were applied to achieve such a modeling. For example, Mosser et al. (2009a) modeled 4 light curves which, except for HD175726, shows intensity variations of the order of 2–3 mmag, comparable to an active Sun. All are relatively rapid rotators ($2.7\,\mathrm{d} \leq P_{\mathrm{rot}} \leq 3.9\,\mathrm{d}$). The high degeneracy of the problem was overcome by imposing a small number (2–3) of starspots per rotation. The methods was tested with simulated light curves that showed the reliability of the results in terms of rotation period and differential rotation for mid-inclined stars (with a risk of under-estimation). Pole-on and edge-on stars appear to be the most difficult cases. However, the method showed its reliability by applying it to sub-series of long time series of the same star and leading to similar results. For example, differential rotation is observed in 3 out of the 4 modeled stars (Figs. IV.3.6 and IV.3.7).

Other attempts to model the light curves of stars in order to extract an information on the presence of starspots were achieved by Lanza et al. (2009b,a, 2010, 2011). These works focus on stars hosting planets: respectively CoRoT-2a, -4a, and -6a. They rely on another method for the light curve modeling, based on the division the star's surface in small elements, each associated to a parameter accounting for the presence of spot or faculae (or no magnetic signature at all). The parameters for each element are fitted in order to reproduce the observed integrated light curve. The application of this method to stars hosting transiting planets allows the inclination angle of the star to be fixed. A striking results of these works is that, as in 3 stars

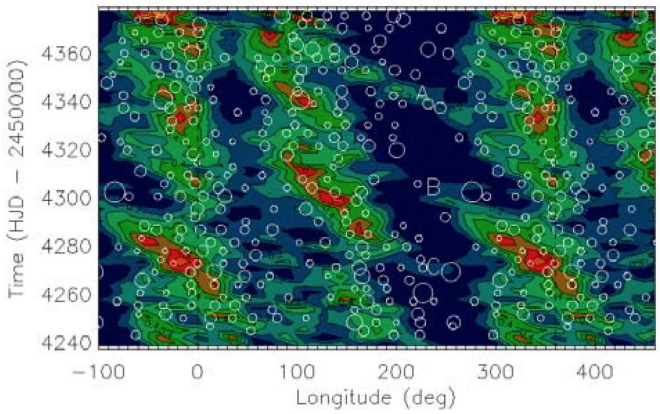

Fig. IV.3.8. Figure 4 of Lanza et al. (2009b), showing (in red and green) the fitted spotted area of CoRoT-2a. The inclined ridges are the signature of the differential rotation. Results of Silva-Valio & Lanza (2011) are superimposed as white circles that represent the spots derived from their independent analysis using the transits of the planet (see text) © A&A.

out of 4 in Mosser et al. (2009a), differential rotation was detected in the 3 planet hosting stars. The measured amplitude of this differential rotation varies from one star to another, from very few percent up to more than 10%. A signature of this differential rotation is visible in the map of the fitted spotted area (Fig. IV.3.8) of CoRoT-2a's star, a young Sun ∼0.5 Gyr old that has been observed for 142 days while the measured rotation period of the star is 4.5 days. The flux modulation of this star is 20 times larger than that of the Sun at maximum of activity. The star hosting CoRoT-2a presents another striking result: the modulation of the measured spotted area with time, which shows an apparent short-term periodicity (Fig. IV.3.9) with a period of $\sim(28.9 \pm 4.8)$ days. This could be the signature of a star-planet interaction[2] as proposed by Lanza (2008) since its period approaches 10 times the synodic period of the planet. This cyclicity could also be compared to the so-called Rieger cycle observed in the Sun (Rieger et al. 1984) which corresponds to a short-term periodicity (154 days) in the occurrence of solar flares, and also in the spotted area (Oliver et al. 1998). A proposed interpretation for this

[2] For more findings about star-planet relations, see Sect. III.9.1

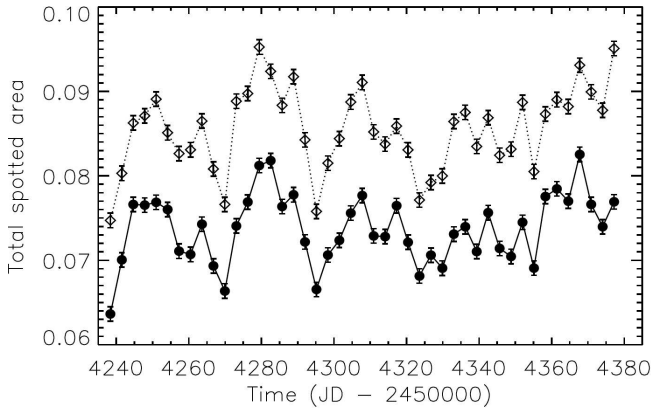

Fig. IV.3.9. Figure 6 of Lanza et al. (2009b), showing the fitted total spot area (for two models) along time. For both models, a clear periodicity is visible © A&A.

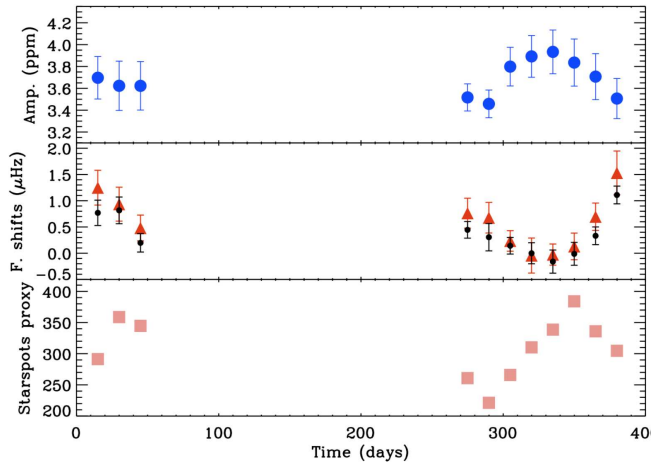

Fig. IV.3.10. Fig. 1 of showing how mode frequencies and amplitudes evolve in an anti-correlated manner for the two first observations of HD49933 by CoRoT. The activity also shows a correlated behavior with a ∼30-day lag © Science, 329, 1032.

oscillation is the propagation of Rossby-type waves in the sub-photospheric layers (Lou 2000).

This star presents also a common feature with the star hosting CoRoT-6a: the presence of active longitudes are observed in the fitted spot map. In CoRoT-2a, two active longitudes are found, 180° apart, with one of them affected by a retrograde migration. In the case of CoRoT-2a, an independent analysis of Huber et al. (2010) as well as another of Silva-Valio & Lanza (2011) (see below) confirmed the presence of these active longitudes. The active longitude detected in the case of CoRoT-6a (an F9 star with a rotation period of ∼6.3 days, observed for 145 days) is even more interesting since it appears to remain at a somewhat constant distance in longitude to the sub-planetary point (with however an important gap: ∼200°). A related observation is made in CoRoT-4a host star: the spotted area, if not showing an active longitude, shows nevertheless its maximum at a constant longitude with respect to the sub-planetary point. However, some caution is necessary since this star was observed for only 58 days.

As stated above, light curve modeling with the aim of mapping spots (or other heterogeneities) is a highly degenerated problem. There is however a case particularly favorable to this modeling: when a planet transits a spotted

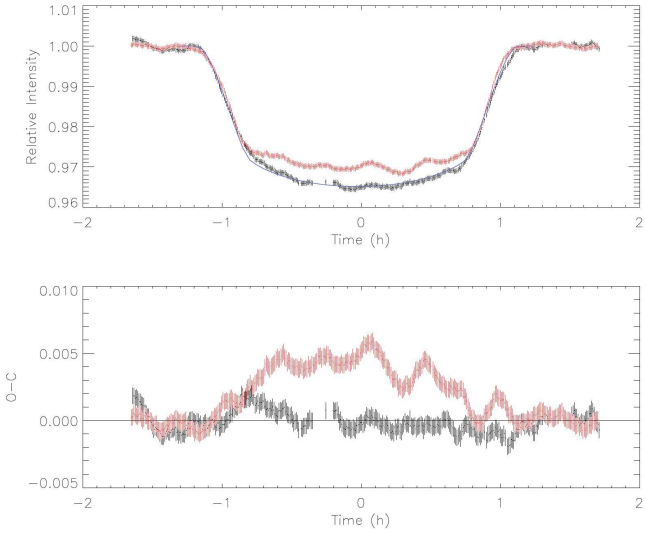

Fig. IV.3.11. Fig. 2 of Silva-Valio et al. (2010), showing the details of a planet transit (CoRoT-2a) during which the signature of occulted spots become visible (red curve) compared to a transit with almost no spot occulted (black curve) © A&A.

stellar photosphere, the details of the light curve during transits is rich in information about the occulted spots. This approach has been developed by Silva-Valio et al. (2010), Silva-Valio & Lanza (2011) in the case of CoRoT-2a. With the hypothesis of a planet orbiting in the equatorial plane, the latitude of the spots can be fixed. The little variations in the light curve during the transit (see Fig. IV.3.11) can be fitted with three parameters: the longitude of the spot, its size (its radius when it is supposed circular) and its intensity. The details of the light curve bring additional information for the determination of the radius, limiting the degeneracy with the intensity of the spot. A first analysis (Silva-Valio et al. 2010) was based on 7 to 9 spots per transit modeling. A second analysis (Silva-Valio & Lanza 2011) used a smaller number (5 spots in average), consequently increasing the average size of the spots from $0.46\,R_p$ to $0.53\,R_p$ (R_p being the radius of the planet). In both cases, it makes the average size of the spots of the order of 100 000 km, several times larger than the largest sunspots. In average, 16.5% of the star surface are covered by spots, confirming that CoRoT-2a star is much more active than the Sun. The re-analysis of Silva-Valio & Lanza (2011) is particularly interesting since the results of Lanza et al. (2009b) for the same star showed the existence of active longitudes. The results of Silva-Valio & Lanza (2011) are superimposed to those of Lanza et al. (2009b) in Fig. IV.3.8 and show an excellent agreement about the spot distribution as obtained by the two different methods, confirming the existence of the active longitudes.

The link between the manifestation of magnetism in surface and the interior of the Sun, evidenced by the frequency shift of acoustic oscillations is well known. The Sun was the only star in which such a link had been observed. One more time, the CoRoT ultra-high precision photometry allowed similar observations in another star, HD49933, in which oscillation frequency shifts were related to surface activity (García et al. 2010). The oscillations of this star behave like those of the Sun: mode frequencies increase when their amplitudes decrease, in correlation with the observed

magnetic activity (see Fig. IV.3.10). Frequency shifts and amplitude variations were measured globally for HD49933 from the two first CoRoT time series of this star (of 60 and 137 days, spanning more than 400 days in total), while the activity was measured through a proxy made from the variance of the intensity variations. This star, rotating much faster than the Sun ($P \sim 3.4$ days), seems to present a much shorter activity cycle, rising in approximately 60 days during the second time series used. As in the solar case, frequencies increase when the activity increases but a time lag of ∼30 days is observed in the case of HD49933. The same authors (Salabert et al. 2011) confirmed their findings by studying the frequency shifts versus frequency for two periods of 90 and 47 days corresponding to a quiet and an active regime respectively. They found a behavior quite similar to that of the Sun, with the frequency shifts reaching their maximum of 2 μHz at 2100 μHz (for HD49933, $\nu_{\max} \sim 1800$ μHz), followed by a downturn at 2300 μHz (and an upturn at higher frequency).

Mathur et al. (2013) looked for the same correlated behavior between modes properties and magnetic activity for three other stars observed by CoRoT (HD49385, HD52265 and HD181420) but did not reach significant results despite using complementary spectroscopic observations (Ca H profiles).

2.3. Another source of micro-variability seen by CoRoT: surface convection

Signatures of magnetic features are not the only ones originating from the photosphere or above and seen in light curves. An important physical process contributes too: the surface convection. The granules induced by this convection have a characteristic time close to the acoustic oscillation periods and thus exhibit power in the Fourier spectra in the form of a continuous background on the top of which the oscillation modes appear as narrow peaks. This background is often modeled as a more or less modified Lorentzian profile $P(\nu)$ centered on the zero frequency, following the initial idea of Harvey (1985) based on the description of a noise process with memory:

$$P(\nu) = \frac{4\sigma^2\tau}{1 + (2\pi\nu\tau)^\alpha}, \quad (1)$$

where σ and τ characterize the height and width of the profile. Harvey (1985) uses $\alpha = 2$ but other authors (*e.g.* Aigrain et al. 2004; Michel et al. 2009) use other values. Ludwig et al. (2009) compared spectra from 3D hydrodynamical simulations to spectra from F stars observed by CoRoT (mainly HD49933, but also HD181420 and HD181906). While the simulated spectra (derived from a solar model) are in agreement with observations of the Sun, some non negligible discrepancies appear between simulated spectra for HD49933 and the observed one. Even if these hydrodynamical models are sensitive to the global characteristics of the star (such as $\log(g)$ or $T_{\rm eff}$), the spectra of HD181420 and HD181906 (which have similar stellar characteristics) are very similar to that of HD49933, suggesting a lack in the hydrodynamical description. Samadi et al. (2013) compared characteristics of the granulation spectra (σ and τ) from grid of models to observed ones (from Kepler) and noted that the largest discrepancies occur for F stars. They suggest that the source of the discrepancies could be the photospheric magnetic field of these stars, following the results of Chaplin et al. (2011) who noted that acoustic oscillations in F stars were the most sensitive to damping by magnetic field. Since oscillation are excited by surface convection, it strongly suggests that a proper description of the effect of magnetic field on convection in the hydrodynamical models is necessary.

3. Binaries (by C. Maceroni)

CoRoT lead to a revolution also in the field of binary stars. The two main assets of the mission, high accuracy and long term monitoring, provided extraordinary data for binary star studies, allowing the detection of effects immeasurable before. Besides, CoRoT made possible a fruitful synergy between asteroseismology and binarity, two independent and complementary sources of information on stellar properties.

Among the bright field targets there were a few known bright eclipsing binaries (EBs), but others were added to this list when their unknown binary nature was revealed by the observations (e.g. HD 174884, see below). In the faint fields EBs resulted to be, as expected, the majority of regular variables.

3.1. Statistical properties of the eclipsing binaries in the faint fields

A complete list of CoRoT eclipsing binaries from the exoplanet fields is in preparation and will be available in Exodat (`http://cesam.oamp.fr/exodat/`) (M. Deleuil, private communication), but several partial lists have been compiled during the mission. So far the most complete and useful for eclipsing binary studies is the CoRoT unofficial online catalog[3] assembled by J. Devor. This catalog provides not only the parameters describing the light curve (orbital period, eclipse depth and duration), but as well the system parameters, as derived by a new algorithm based on JKTEBOP eclipsing binary model (Popper & Etzel 1981; Southworth et al. 2004) and Markov Chain Monte Carlo (MCMC). A full analysis of this data set will appear elsewhere (Devor et al., in prep.), we use here some of the online data for a first look at the orbital period distribution.

The catalog contains the eclipsing/ellipsoidal binaries detected in the initial run (IRa01), in eleven long runs (LRc01...LRc06, LRa01...LRa05) and five short runs (SRc01, SRc02, SRa01...SRa03) for a total number of 1437 systems. Some of the selected objects, however, had doubtful classification because of the difficulty in discriminating, with an automatic algorithm and on the basis of a single light curve, between light variation due to low-inclination ellipsoidal systems and that due to surface spots or pulsation. We performed, therefore, a manual vetting of the curves which yielded a "bona fide" sample of 1142 binaries.

The binary frequency in the observed fields has a mean value of $0.9 \pm 0.2\%$, i.e. about twice the frequency obtained from large ground-based surveys (e.g. OGLE). That is due to the long term monitoring and high accuracy of CoRoTphotometry, which allows to detect systems difficult to discover from the ground.

[3] `www.astro.tau.ac.il/~jdevor/CoRoT_catalog/catalog.html`

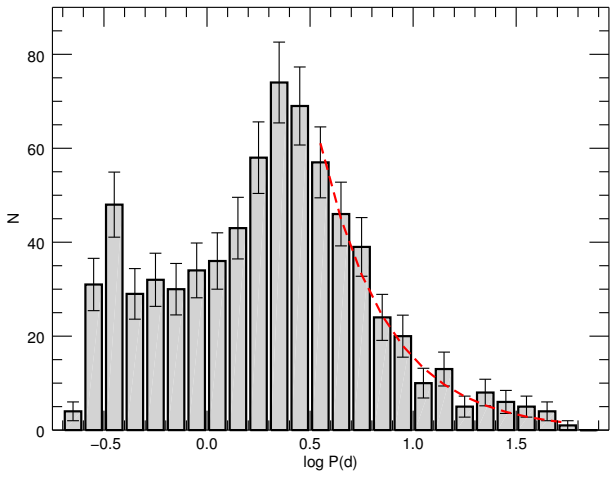

Fig. IV.3.12. Period distribution of the bona fide sample. The error bars are derived from the Poisson statistics uncertainties based on the number of systems. The red broken line is an estimate of the effects of discovery selection according to Maceroni & Rucinski (1999) © A&A.

The orbital period distribution of the "bona fide" sample is shown in Fig. IV.3.12. The secondary peak at short period is a well known feature and is generally attributed to the effect of secular evolution producing orbit shrinking in wider binaries. That can be due to angular momentum loss, due to magnetic braking of wind, in synchronized solar-type binaries (Vilhu 1982; van't Veer & Maceroni 1989), and/or to the Kozai mechanism in triple systems (Kozai 1962; Fabrycky & Tremaine 2007). The drop after maximum is essentially due to the decrease of the probability of eclipse with increasing period, because of the reduced range of inclinations producing eclipses. Moreover, the tail of the distribution is affected by the run duration (varying from ∼160 d to ∼80 days for long runs and from ∼60 to ∼30 days for the initial and the short runs). For illustrative purpose, the dashed line is the expected observed distribution of EBs from a population of binaries with a flat log P distribution. The curve corresponds to a selection effect proportional to $P^{-4/3}$, according to a simplified computation proposed by Maceroni & Rucinski (1999). Their simple estimate computes the probability that a distant observer notices eclipses by evaluating the solid angle subtended by the sum of the fractional radii (R/a, with a the system semi-axis) relative to visible hemisphere, i.e., by dividing it by 2π sr. This relative solid angle is given by the integral of the eclipse relative durations over the range of inclinations that can result in eclipses. The same proportionality is obtained by considering the fraction of the sky that one star 'sees' covered by the companion. If it is assumed that the range of variation of the sum of the component radii is much smaller than that of the orbital separation, this probability scales as a^{-2} and hence $P^{-4/3}$. The displayed curve is the best fit, with fixed exponent, to the distribution for $\log P > 0.5$.

Figure IV.3.13 shows the period distribution of subsamples, according to the galactic coordinates. Panel a) shows the distribution dividing the whole sample according to the direction (Center and Anticenter). The former has a more marked bimodal distribution, with a larger fraction of systems in the short period bins. A Kolmogorov-Smirnoff test of the hypothesis that the two samples are drawn from the same population yields a very low probability $KS = 0.0018$. The difference could be an indication of an older population in the direction of the galactic center fields, as that will imply a larger fraction of low-mass components (which can accomodate in a smaller orbit) and a longer time for efficient shrinking of the orbit.

This indication is in qualitative agreement with the results of differential population studies by means of oscillating giants (Miglio et al. 2013) in the first CoRoT long runs (LRa01 and LRc01). According to their analysis the sample of giants in LRc01 is characterised by a lower mean mass and higher age than that in the opposite direction. The fields considered in their study, however, have different galactic latitude, b, ($b \simeq -8$ for LRc01 and $b \simeq -2$ for LRa01) and a difference in b could also be a factor modifying the distributions.

To disentangle the effect of galactic latitude and longitude on the distribution, samples from fields of similar latitude or longitude are compared in the other panels. All the distribution pairs have a low value of KS. Evidently, an higher percentage of shorter period binaries appears in the higher latitude fields for both center and anticenter directions, and, as well, in the center direction with respect to the anticenter.

We also checked if the effect could also be related to the different amount of interstellar absorption, which is rather different and patchy in the various fields. To this purpose we used the population synthesis code TRILEGAL (Girardi et al. 2005) to compute the expected distribution of mass and age in the different CoRoT fields, using the reddening maps of Schlafly & Finkbeiner (2011). We also checked the effect on the results of varying A_V, the total absorption along the line of sight, of the same field. The details will be published elsewhere, but in general we can say that higher absorption provides slightly older and less massive "observed" samples and hence, indirectly, a larger number of shorter period binaries, because of the above mentioned mechanisms (angular momentum loss in spin-orbit synchronised solar-type binaries and Kozai mechanism in triple systems). Looking at panels b) and c) of Fig. IV.3.13 we see instead that the distribution is more bimodal, with a secondary peak in the period domain typical of contact binaries, in the high-b fields, where the average absorption is lower. We can conclude, therefore, that the effect is due to a difference in population.

The situation is less clear when comparing the distributions in the d) panel (LRc versus LRa high-b fields), where one probably sees the combination of two effects working in the same sense: the simulations suggest indeed older population for the LRc fields, which however have, as well, a higher average interstellar absorption. The difference in the population properties should be, however, the main reason of the different distribution shape, because the simulations show that the effect of absorption is a secondary one, even in presence of strong variations.

3.2. New binary types

The in-depth study of a number of CoRoT eclipsing systems lead to many discoveries. The accuracy played a fundamental role in the detection of new variable types, the monitoring with dense sampling over several months allowed to follow processes evolving on different timescales, from minutes to hundred days.

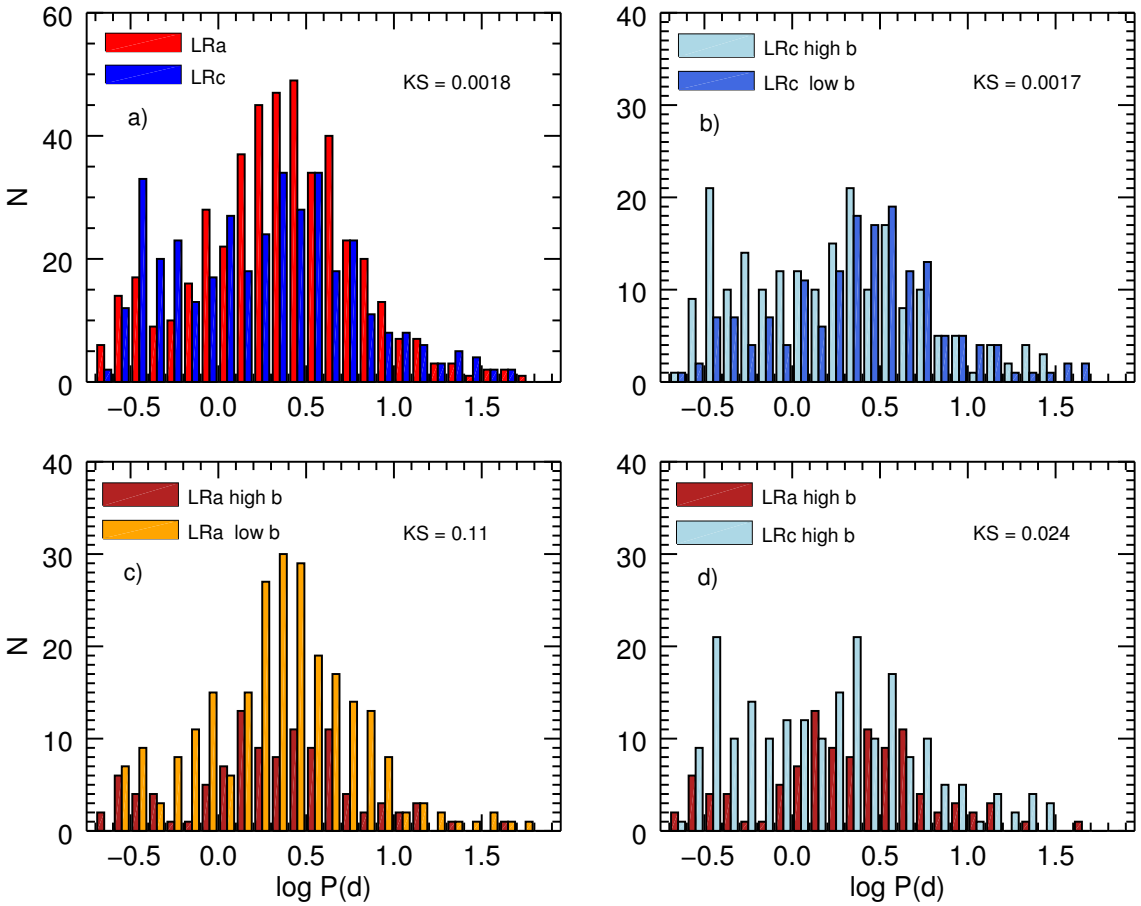

Fig. IV.3.13. The orbital period distribution of different EB subsamples. Panel **a)**: LRa and LRc indicate, respectively, the fields in the CoRoT Anticenter and Center directions. *Other panels*: the high and low galactic latitude refer to fields with galactic latitude absolute value $|b| > 5$ and ≤ 5.

CoRoT photometry discovered several beaming binaries, as predicted before the launch by Zucker et al. (2007) and first observed in the light curve of a *Kepler* target, KIC 7975824 (KPD 1946+4340) (Bloemen et al. 2011). These binaries show minute flux variations due to relativistic beaming (of the order of a few hundred ppm for systems with orbital period of 10–100 days and late-type components). Beaming (also called Doppler beaming or boosting) is due to the star radial velocity (RV): because of the motion the spectrum is shifted in wavelength, the photon emission rate is modulated, and the photons are slightly beamed in the direction of motion (light aberration). The resulting tiny light variation contains information on the radial velocity of the components. Beaming is, however, a subtractive effect, being the radial velocity of the components in anti-phase. Effects of opposite sign sum up weighted by the component fluxes, so that the effect strength is larger in binaries with components of very different flux (where, in practice, beaming from only one star is measured) and is null for identical components. In the most favourable case the analysis of the beaming effect in a light curve allows to extract the RV curve of the brighter component, but more frequently only its RV amplitude. Beaming provides the same information of a single-lined spectroscopic binary, with the advantage of a less demanding effort in terms of observing time. Moreover, beaming allows to discover non-eclipsing binaries from photometry alone. The example is the discovery of seventy-two non-eclipsing binaries from CoRoT light curves by Tal-Or et al. (2015). These are short period non-eclipsing binaries discovered thanks to the combined effect of beaming, ellipsoidal variations and reflection.

The beaming effect was invoked to interpret the unequal height of light-curve maxima (the so-called O'Connell effect) in CID 105906206 (da Silva et al. 2014). The system is a short period ($P \simeq 3^{\rm d}.69$) totally eclipsing detached binary, with a δ Sct primary component. The asymmetry of light-curve maxima appeared after pre-whitening the light curve with more than 200 frequencies found by using a harmonic analysis. The detached configuration, the stability of the feature over 160 days (and ∼50 rotation cycles being the system components close to corotation), and the agreement of the beaming parameters with the radial velocity amplitude suggested the interpretation of the feature as due to beaming.

Another recently defined class of binaries is that of Heartbeat binaries (HBB). These are short period systems characterized by a strongly eccentric orbit and ellipsoidal light variation. The name derives from the unusual light-curve shape which, in non-eclipsing systems, recalls that of ECG tracings. In this case the light curve shows a single variation around periastron due to surface deformation and mutual irradiation of the components. The presence of tidally induced pulsation in the light curve is another distinctive property.

The shape of the HBB light curve was theoretically predicted by Kumar et al. (1995). The iconic heartbeat binary

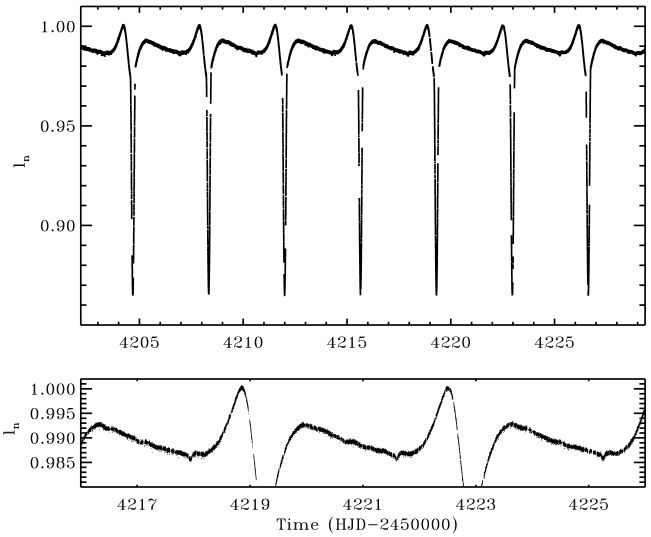

Fig. IV.3.14. *Upper panel*: the complete CoRoT light curve of HD 174884 as normalized flux vs HJD. *Lower panel*: a blow-up, spanning approximately three periods, showing the tiny secondary minimum (first occurrence at reduced HJD of around 4218). Reprinted from Astronomy and Astrophysics (Maceroni et al. 2009) © A&A.

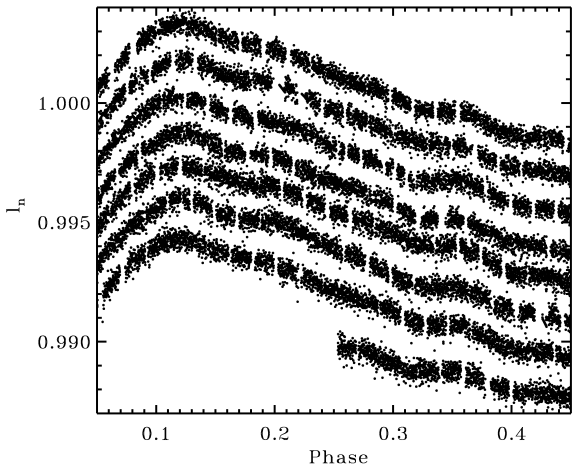

Fig. IV.3.15. Sections of the original light curve of HD 174884, phased according to the orbital period of 3.657 days and vertically shifted for better clarity. The seven observed orbital periods go bottom-up. An quasi regular pattern can clearly be seen in each curve. Reprinted from Astronomy and Astrophysics (Maceroni et al. 2009) © A&A.

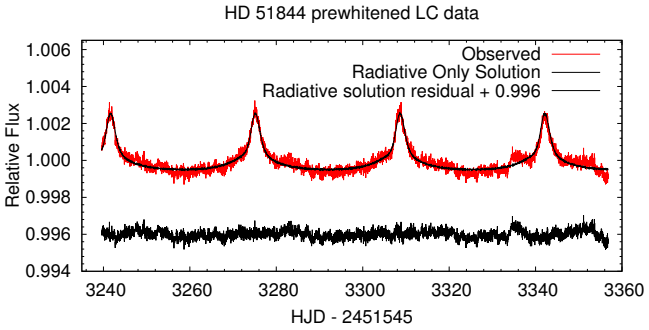

Fig. IV.3.16. The periastron brightenings in the light curve of HD 51844 and the corresponding best fit. Reprinted from Astronomy and Astrophysics (Hareter et al. 2014) © A&A.

is the *Kepler* target KOI-54 (Welsh et al. 2011) which was the first announced system of the class; more than hundred heartbeat binaries were discovered afterwards among the *Kepler* targets (Hambleton et al. 2013).

The original criteria for HBB definition excluded eclipsing systems, but this restriction was dropped afterwards (Hambleton et al. 2013), considering that eclipse is only an aspect-dependent event. With this broader definition the ante-litteram example of heartbeat systems is actually a CoRoT target: the eclipsing binary HD 174884, (Maceroni et al. 2009) whose light curve is shown in Fig. IV.3.14. The system is formed by two late B stars and the difference in depth between the two minima (the secondary depth is 1% of the primary) is entirely due to the high eccentricity ($e \simeq 0.3$) and the orientation of the orbit with respect to the observer. The pulsation analysis on the residual curve, after removal of the binary signal, revealed the presence of overtones of the orbital frequency, which can actually even be spotted by eye in the original curve (Fig. IV.3.15) and were interpreted as tidally induced pulsations.

A more classical HBB is HD 51844 (Hareter et al. 2014), a double-lined spectroscopic binary with a δ Sct component of spectral type Am. The system has an orbital period of 33.498 days, a high eccentricity ($e \simeq 0.48$) and is formed by almost twin components of mass $\simeq 2\ M_{\odot}$. In spite of that, only one star (the secondary) pulsates with measurable amplitude. The fact that similar stars exhibit completely different stability against pulsation is not new: only a fraction of field stars in the δ Sct instability strip of the HR diagram pulsates. When, however, the twin stars are components of close binaries, the conclusion is that the pulsational properties can significantly differ even for stars of the same age and chemical composition, which poses a challenging problem to theory.

The periastron brightening of the light curve of HD 51844 (Fig. IV.3.16) allowed to constrain the binary model even in absence of eclipses. Additional remarkable findings of this investigation are the high overtones of the orbital period in the frequency spectrum (interpreted as tidally induced pulsations) and the discovery of resonances, found for the first time in a δ Sct star.

3.3. Case studies

CoRoT offered for the first time the possibility of combining in an effective way the information coming from duplicity and from pulsation, thanks to the continuous monitoring of a large number of targets. When the pulsating stars belong to a binary there is an independent way of determining the component absolute parameters. This is of fundamental importance for asteroseismic studies as it allows to constrain the component modeling. A few cases have already been described in the previous section, but other are worth mentioning for the new insight offered by the synergy with asteroseismic studies.

Only one eclipsing system with a γ Dor component was known before CoRoT launch (VZ CVn, Ibanoğlu et al. 2007) but its sparse photometry from ground did not allow to really exploit the combination of eclipses and pulsations. CoRoT discovered a number of γ Dor pulsators

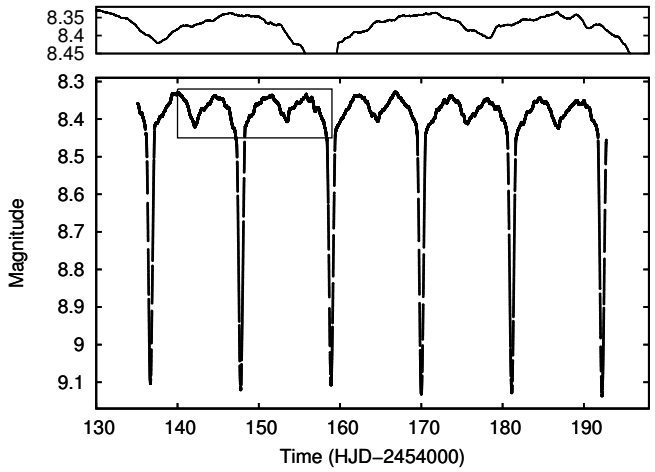

Fig. IV.3.17. The complete CoRoT light curve of AU Mon. The *upper panel* shows an enlarged segment of the curve with very clear rapid non-orbital variations. Reprinted from Monthly Notices of the Royal Astronomical Society (Desmet et al. 2010) © Monthly Notices of the Royal Astronomical Society.

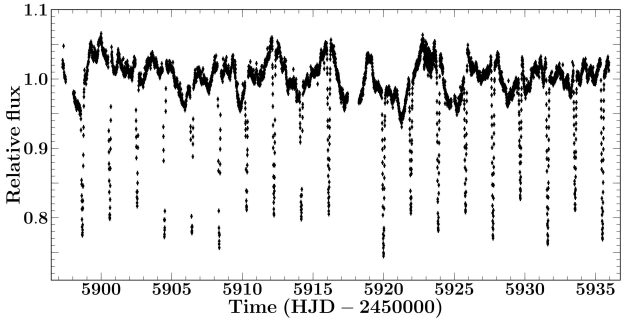

Fig. IV.3.18. The light curve of CID 223992193 as obtained by CoRoT in the run SRa05 (December 2011/January 2012), the system was observed also during the short run SRa01 (March 2008). Reprinted from Astronomy and Astrophysics (Gillen et al. 2014) © A&A.

in EBs (Sokolovsky et al. 2010; Maceroni et al. 2013) including hybrid γ Dor/δ Sct (Chapellier & Mathias 2013) and a possible detection in a triple system (Dolez et al. 2009). In addition, CoRoT made possible to investigate seismically unexplored regions of the HR diagram, such as that of very massive stars: the investigation of the young O-type binary HD 46149 (a double-lined spectroscopic binary Degroote et al. 2010) evidenced the presence of solar-like oscillations in a massive O-type star, while that of HD 50230 (Degroote et al. 2012) revealed a a prototypical hybrid pulsator in a B-type wide binary and allowed to put constraint on the component internal structure (Degroote et al. 2010).

The continuous monitoring over months and the dense sampling of the light curve offered as well the opportunity to study in depth binary systems with a complex configuration and presenting variability on different time scales. An example is the analysis of the eclipsing binary AU Mon (Desmet et al. 2010), a strongly interacting Be + G semi-detached system with an orbital period of ∼11.11 days, whose light curve is shown in Fig. IV.3.17. In addition to eclipses, the study evidenced variability on a long time scale ($416^{\rm d}$), which was detected by combining of the CoRoT light curve (spanning $56^{\rm d}$) with pre-existing photometry of the system. The variability was interpreted in terms of matter surrounding the mass exchanging components and, thanks to eclipse mapping, modeled as an accretion disc by Mimica & Pavlovski (2012). Afterwards, a complementary investigation, based on optical and archival UV spectroscopy, evidenced the presence of a stream+disc+bright-spot around the Be primary (Atwood-Stone et al. 2012). The CoRoT photometry showed, as well, additional periodic variability (on a scale of a tenth of a day) which was interpreted as due to non-radial pulsations of the Be star. To be noticed that the corresponding frequencies are not predicted by theory but were observed in other CoRoT Be targets (as HD 49300, Huat et al. 2009). Finally, the Scargle periodogram of the CoRoT light curve is characterized by a power excess in agreement with solar-type pulsations of the G-type component.

Another complex and rare system is CID 223992193 (Gillen et al. 2014), a detached EB formed by two pre-main sequence dwarfs ($P_{orb} \simeq 3\overset{\rm d}{.}84$). The detailed modelling of the large amplitude out-of-eclipse variations (Fig. IV.3.18) combined to that of high-resolution spectroscopy and of the infrared SED revealed the presence of dust in the inner cavity of a circumbinary disc. The small amount of dust necessary to explain the out-of-eclipse variations could be present in the accretion streams from the disc itself.

Finally unusual binaries were detected as by-products of planet transit search, which ended sometimes in the serendipitous discovery of rarely observed binary systems, as for CID 110680825 (CoRoT LRa02_E2_0121, Tal-Or et al. 2011). In this case a Neptun-sized planet candidate target turned out to be a hierarchical triple system formed by a far giant primary and a grazing eclipsing binary of orbital period $\simeq 36\overset{\rm d}{.}3$. The inner system is formed by A- and F-type components. The reason for the false positive planet detection is dilution of the inner-binary light curve by the light of the giant companion, mimicking a less deep transit. A very sophisticate analysis allowed to detect also a tiny secondary minimum, only 0.07% deep, and to characterise the system, which is the second known of this type after HD 181068 (Derekas et al. 2011). The original light curve and the minima of the phase-folded one are shown in Fig. IV.3.19.

Similarly, the study of the transit candidate CID 101186644 (Tal-Or et al. 2013) revealed a strongly eccentric eclipsing binary with a period of ∼20.7 days. The interesting system component is in this case a low-mass, dense late M-dwarf secondary, the smallest and densest detected so far ($R = 0.104\ R_\odot$, $M = 0.096\ M_\odot$). The detection is important because of the small number of stars in the region of very low mass stars ($M < 0.2\ M_\odot$). At variance with most other similar objects this M-dwarf has a radius in agreement (or perhaps even smaller) than that predicted by theoretical models. Its discovery weakens, therefore, the claim that low-mass star are larger than predicted by evolutionary models.

In conclusion CoRoT provided a rich harvest of scientific results in the field of binary stars and certainly much more will come from the exploitation of its legacy archive.

4. Stars with disks (by S.H.P. Alencar)

Disks are ubiquitous to the star formation process. They are the sites of planet formation and may interact with

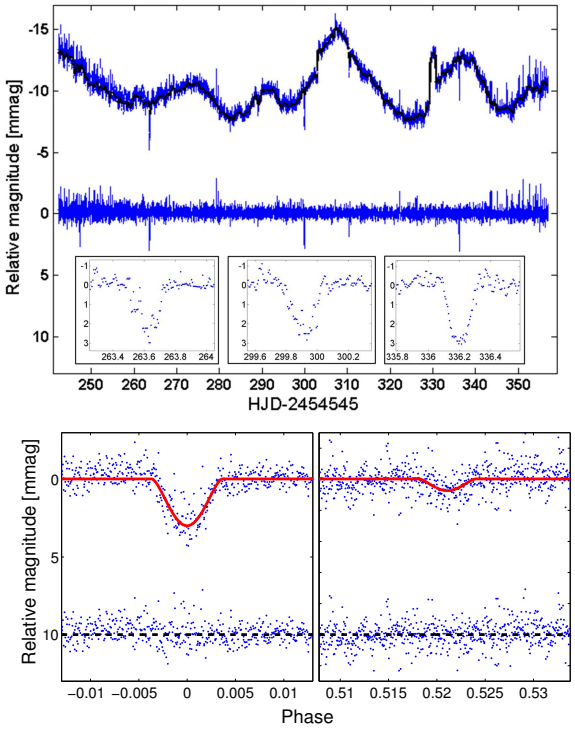

Fig. IV.3.19. *Upper figure*: The white light curve of CID 110680825. Top: the calibrated light curve (up-shifted by 10 mmag) after rebinning and removal of outliers; the long-term trend is overplotted in black. Middle: the detrended light curve. Insets: zoom on the three individual transit-like events. *Lower figure*: the primary and secondary eclipses in the phase-folded light curve with the best model overplotted with a solid red line. The residuals are downshifted by 10 mmag. Reprinted from Astronomy and Astrophysics (Tal-Or et al. 2011) © A&A.

the central star through the stellar magnetic field. T Tauri stars are low ($M \leq 2\ M_{\odot}$) mass stars of a few million years. Many of them, called classical T Tauri stars (CTTSs), still present accretion signatures from a circumstellar disk (Ménard & Bertout 1999). Understanding the accretion process acting in the star-disk system and disk evolution are some of the major challenges in the study of star formation nowadays. Accretion has a long and important impact in the initial evolution of low mass stars, regulating its fundamental properties (mass and angular momentum), and some of its most remarkable features (energy excess with respect to stars of the same age and mass that no longer accrete and mass loss through collimated jets). The discovery of thousands of extrasolar planets in the last decades has increased the importance of the evolution and dissipation of accretion disks around young stars, since they directly impact the study of planetary formation. The characterization of the accretion process in young stellar systems and their disks is therefore an important step to the establishment of credible scenarios of star and planet formation.

In young low-mass stars, magnetic fields can reach several kilogauss (Johns-Krull et al. 2001), causing the truncation of the inner disk region and directing the accreting material towards the star. The magnetospheric accretion process leads to the development of magnetic accretion columns that extend from the inner disk regions, at a few stellar radii from the star, to the stellar surface, originating accretion shocks at the surface of the star, where the accreting, nearly free-fall, material is rapidly decelerated (Bouvier et al. 2007b). The stellar magnetic field is also responsible for the transfer of angular momentum from the star to the disk, allowing the young accreting systems to rotate well below break-up velocity, despite the accretion and contraction processes at work (Affer et al. 2013; Gallet & Bouvier 2015). These various components (inner disk structure, accretion columns and shocks) are not directly observable due to our distance to star forming regions, but they generate spectral and photometric features that can be analysed to understand the accretion and outflow flux structure and its dynamics.

4.1. First CoRoT observations of NGC 2264

The CoRoT satellite allowed the observation of additional programs in short runs, not necessarily related to its main objectives of finding exoplanets and studying astroseismology. The first additional program completed by CoRoT, in 2008, was the 23-day continuous observation of NGC 2264, a young (∼3 Myr) stellar cluster located at about 760 pc from the Sun (Dahm 2008). This was the only young cluster in the CoRoT "eyes" and a unique opportunity to study young stars with precise and high-cadence photometry. The CoRoT data on NGC 2264 yielded the most exquisite light curves ever obtained of young star-disk systems and originated very detailed analysis of variability in these systems. This initial campaign provided clues on the relation between accretion and X-ray variability (Flaccomio et al. 2010), it allowed the study of the circumstellar structure of accreting systems (Alencar et al. 2010), rotation in the Pre-Main Sequence (Affer et al. 2013), pulsations in young intermediate mass stars (Zwintz et al. 2013), and several young eclipsing binary systems were also discovered (Gillen et al. 2014).

Alencar et al. (2010) analysed the light curves of all the classical T Tauri stars of NGC 2264 observed by CoRoT and classified them in three simple categories: spot-like, which are periodic light curves dominated by variability due to starspots, AA Tau-like, periodic light curves whose variability is due to extinction by circumstellar dust, and irregular, which includes all the non-periodic light curves (Fig. IV.3.20). They showed that the highly dynamical star-disk interaction mediated by the stellar magnetic field observed in the classical T Tauri star AA Tau (Bouvier et al. 1999, 2003, 2007a) is apparently common among CTTSs ($28\% \pm 6\%$ of CTTSs in their sample presented AA Tau-like light curves). AA Tau-like light curves are observed in high inclination systems with respect to our line of sight and the light curves are dominated by extinction due to circumstellar material located at the inner disk edge. The interaction of the stellar magnetic field with the inner disk creates a warp that occults the star as the system rotates. The observed minima typically vary at each rotational cycle (Fig. IV.3.20), implying that the star-disk interaction and the inner disk structure is dynamic on a rotational timescale. Alencar et al. (2010) also showed that the inner disk warp is located close to the disk corotation radius, by comparing the period distribution of AA Tau-like systems and spot-like ones, the latter ones necessarily corresponding

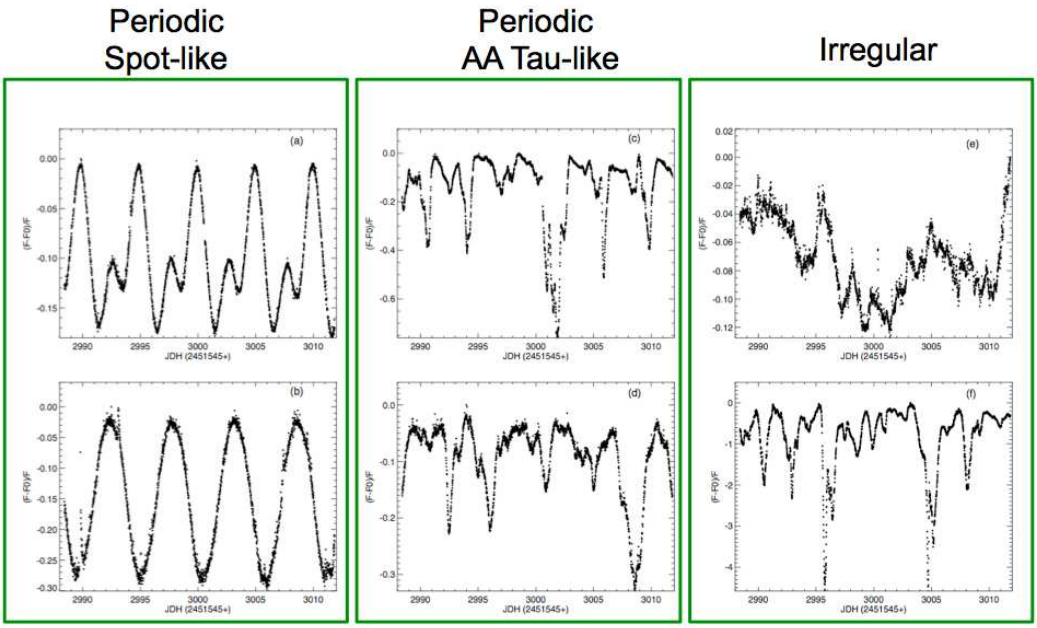

Fig. IV.3.20. CoRoT light curves of classical T Tauri stars, showing different morphological types. Spot-like light curves are periodic and due to spots at the stellar surface. AA Tau-like light curves are also periodic and due to obscuration of the central star by an inner disk warp. The irregular light curves include accretion-burst systems **(e)**, non-periodic circumstellar dust distribution **(f)** and light curves that are not clearly dominated by a unique physical process. Figure adapted from Alencar et al. (2010) © A&A.

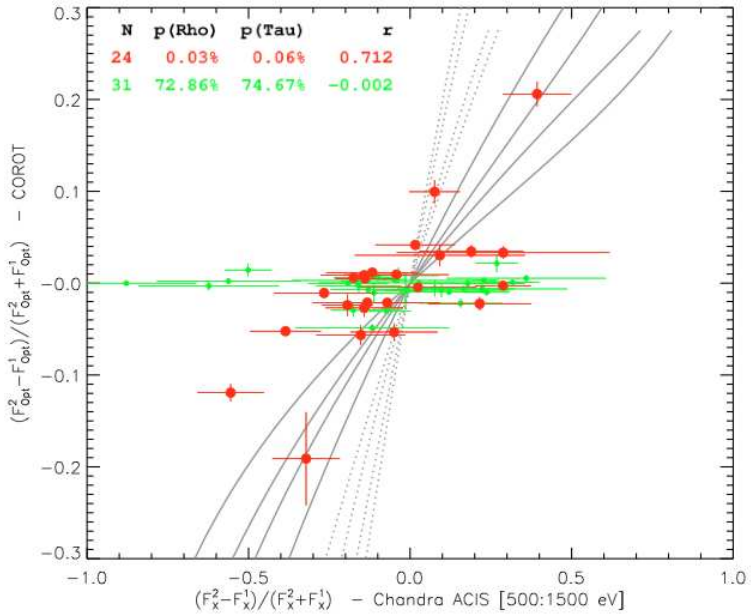

Fig. IV.3.21. Optical and soft X-ray variability for the WTTSs (green points) and CTTSs (red points) of NGC 2264 observed by CoRoT and Chandra. The lines indicate the effect of absorption on a constant source with average $A_V = 1.0$, assuming a standard interstellar gas/dust ratio (dotted lines), and a 5 times higher gas/dust ratio (solid lines). The four lines in each set refer to the combinations of two plasma temperatures, 0.6 and 5.0 keV, and two different assumptions for the spectrum-dependent extinction law in the wide CoRoT band: $A_{CoRoT}/A_V = 1.0$ and $A_{CoRoT}/A_V = A_I/A_V = 0.61$. Figure from Flaccomio et al. (2010) © A&A.

to the stellar rotation periods, since the spots are located at the stellar surface.

Flaccomio et al. (2010) showed that, for CTTSs, soft-X-ray (0.5–1.5 keV) and optical variabilities were correlated (Fig. IV.3.21), while no correlation was found between optical and hard X-rays (1.5–8.0 keV), or between optical and either soft or hard X-rays for the non-accreting weak line T Tauri stars (WTTSs). The observed correlation was explained in terms of variable absorption from circumstellar material, in a scenario similar to the one proposed for AA Tau-like systems. The slope of the observed correlation implies a significant dust depletion in the circumstellar

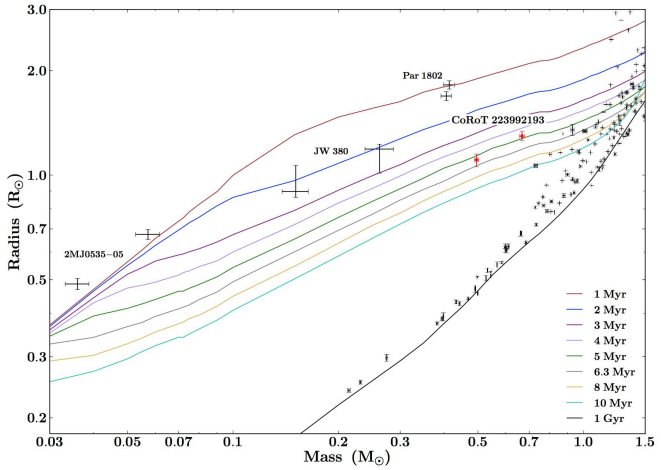

Fig. IV.3.22. Mass-radius relation for the three lowest-mass eclipsing binaries known in the Orion Nebula Cluster (black points) and CoRoT 223992193 (red points) compared with theoretical isochrones of Baraffe et al. (1998) with $Y = 0.282$, [M/H] = 0 and mixing length $\alpha = 1.9$. Figure from Gillen et al. (2014) © A&A.

material (gas/dust ratio ∼5 times higher than the standard value for interstellar material).

Affer et al. (2013) presented a detailed analysis of the period distribution of all the CoRoT observed members of NGC 2264. They showed that CTTSs rotate slower than the WTTSs (Fig. IV.3.2), as also observed by other authors (Lamm et al. 2005; Cieza & Baliber 2007). This agrees with the proposed disk-locking scenario (Shu et al. 1994; Hartmann 2002), in which the interaction between the stellar magnetic field and the inner disk is able to transfer angular momentum from the star to the disk, despite the ongoing accretion and contraction.

Some eclipsing binary systems were discovered with the CoRoT observations of NGC 2264 and the most promising ones are being followed-up. CID 223992193 was the first binary system analysed from the sample and turned up to be a very interesting double-lined, detached eclipsing binary, composed of two young M dwarfs, possibly surrounded by a circumbinary disk from which the young stars may still be accreting (see Sect. 3.3 as well as Figs. IV.3.18 and IV.3.22 and Gillen et al. 2014). This binary system allows to test evolutionary models in a region where only a few stars are known and may also constitute a good laboratory to understand accretion from circumbinary disks.

4.2. The Coordinated Synoptic Investigation of NGC 2264

In December 2011, a new multiwavelength observational campaign of NGC 2264, called the *Coordinated Synoptic Investigation of NGC 2264* (CSI 2264), was organised. It included 40 days of continuous and simultaneous optical photometric observations with the CoRoT and MOST satellites, 30 days of infrared (IR) photometry with the *Spitzer* satellite and 3.5 days of X-ray observations with the Chandra satellite (Cody et al. 2014). Eleven ground-based telescopes were also involved in the campaign, providing, among other data, u-band observations with Megacam/CFHT and 20 epochs of VLT/FLAMES in two cluster fields. Very precise optical, 3.6 and 4.5 μm light curves were obtained for nearly 500 NGC 2264 members, about a third of which are accreting star-disk systems. The wealth of data from CSI 2264, combined with the 2008 campaign, permitted to probe young stellar systems variability in different timescales, from minutes to years, with optical and IR photometry of very high quality.

The CSI 2264 campaign demonstrated the diversity of the photometric behaviour of classical T Tauri stars and showed that 81% of the disk-bearing stars were variable in the optical and 91% in the mid-infrared. The CTTS light curves could be grouped in seven different variability classes, according to a light curve morphology analysis based on metrics of periodicity, stochasticity, and symmetry, that were associated with different physical processes and system geometries (Fig. IV.3.23 and Cody et al. 2014). The data are consistent with variability due to variable circumstellar obscuration, unsteady accretion, rotating starspots, and rapid structural changes in the disk, but sometimes more than one process could be acting simultaneously. Cody et al. (2014) showed that periodical and aperiodical optical dippers constitute the largest variability category (21% of the variable sample), and that the optical and IR variability were not correlated in over 50% of the observed systems (Fig. IV.3.24).

The spatial association between the inner disk warp caused by the stellar magnetosphere, the accretion columns along magnetic field lines and the accretion shock, that was previously only demonstrated for the classical T Tauri star AA Tau (Bouvier et al. 2007a), was confirmed for the stars with periodic and aperiodic extinction events ("dippers") in NGC 2264 (Fonseca et al. 2014; McGinnis et al. 2015). Average values of inner disk warp maximum height of 0.23 times its radial location were found, consistent with AA Tau, with variations on average of 11% between rotation cycles, indicating a very dynamical star-disk interaction.

Short duration, narrow flux dips associated with circumstellar material lifted up above the disk midplane were observed in the CoRoT and *Spitzer* light curves of a few systems (Stauffer et al. 2015). These narrow flux dips can be associated with dust in the inner disk region and the accretion funnel. Some of the narrow dips were periodical and occured superposed on sinusoidal variariations due to cold spot at the stellar photosphere, like in the light curve of Mon-21 (Fig. IV.3.25). Since both variabilities presented the same period, it confirms that, at least in this case, the stellar rotation rate is locked to the Keplerian rotation period at the inner disk, a long debated theoretical prediction (Koenigl 1991; Collier Cameron & Campbell 1993).

A well populated class of young stars with accretion-burst light curves was observed in detail for the first time (Fig. IV.3.26 and Stauffer et al. 2014). This type of systems were predicted by magneto-hydrodynamic simulations (Kulkarni & Romanova 2008), but difficult to find due to their rapid variability. Typically, optical and infrared bursts last from several hours to one day, with amplitudes of about 5%−50% the quiescent value. The high cadence of the CoRoT and *Spitzer* observations allowed the identification of several burst systems, whose variability arises from enhanced mass accretion rates, as confirmed by their high UV excess and very strong Hα emission lines.

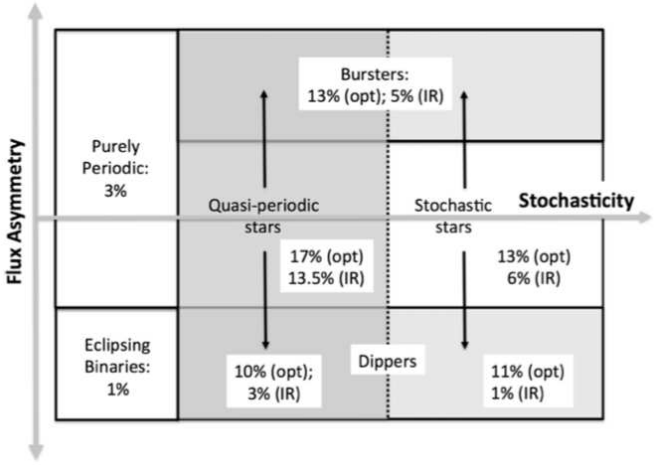

Fig. IV.3.23. Distribution of optical and IR light curves among the different light curve classes. © The Astronomical Journal, 147, 82.

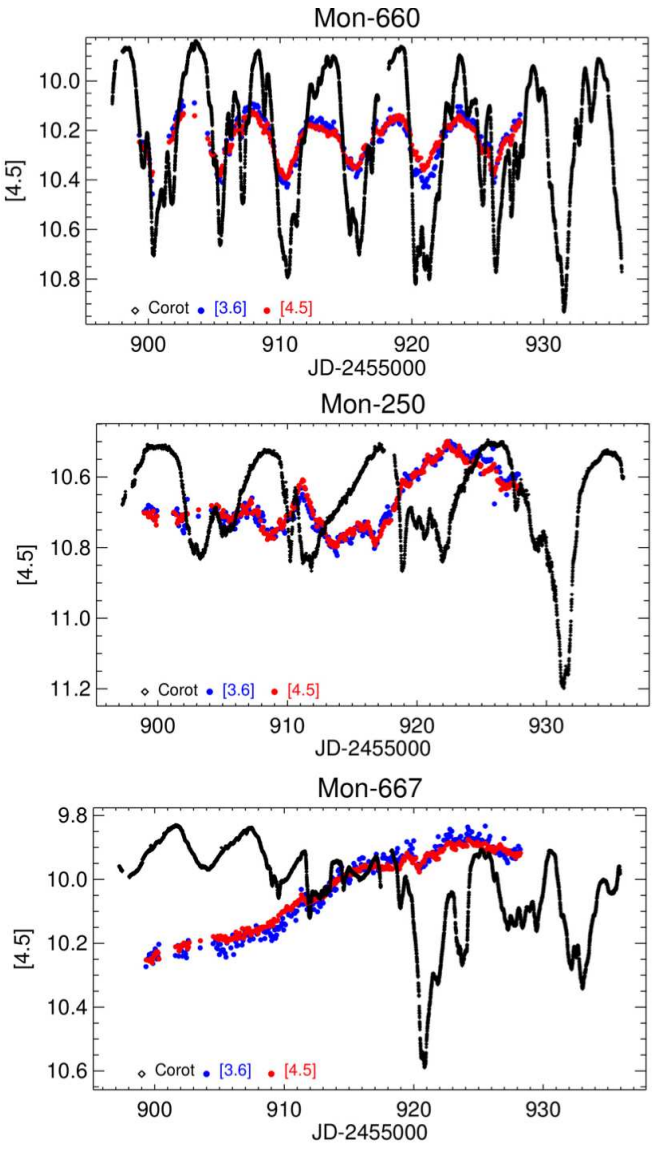

Fig. IV.3.24. Simultaneous CoRoT and *Spitzer* light curves of CTTSs in NGC 2264 that show different degrees of correlation. The top panel shows a system that presents very well correlated optical and IR light curves. The middle panel presents a system where the optical and IR variations are almost anti-correlated, while the bottom panel shows a CTTS that presents no correlation between the optical and IR light curves. Figures from McGinnis et al. (2015) © A&A.

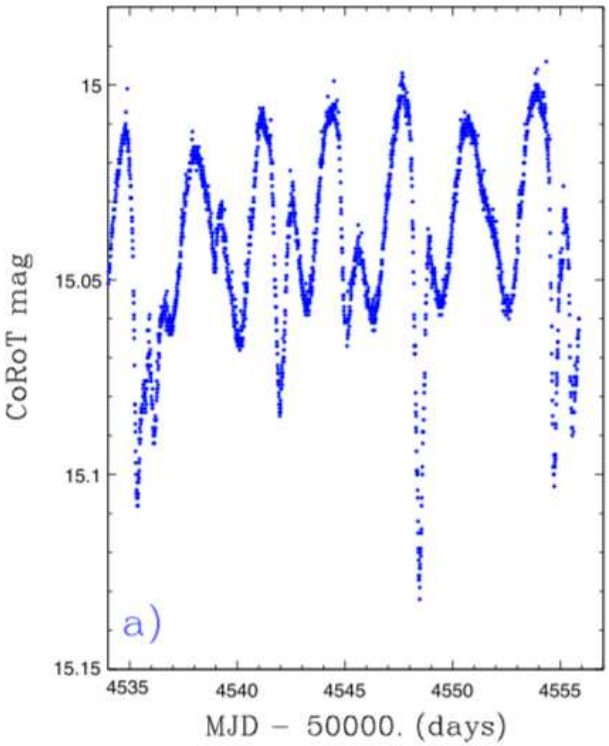

Fig. IV.3.25. CoRoT light curve of Mon-21 that shows spot-like sinusoidal variations with narrow dips due to circumstellar material superposed. © The Astronomical Journal, 149, 130.

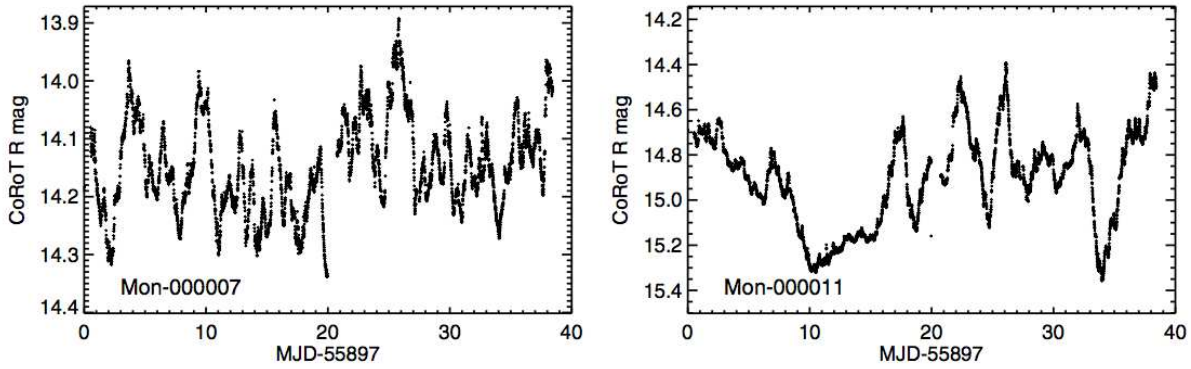

Fig. IV.3.26. CoRoT light curves of CTTSs that show accretion bursts. © The Astronomical Journal, 147, 83.

The association between accretion and inner disk evolution was demonstrated and is related to the morphology of the CoRoT light curves (Sousa et al. 2015). Accretion burst systems present high mass accretion rates and thick inner disks, the AA Tau-like systems show intermediate mass accretion rates and have disks in the transition region between thick to anemic, while most Classical T Tauri stars with spot-like light curves present low mass accretion rates and low mid-infrared excess. Accretion was observed to be highly dynamic and to occur in stable and unstable regimes, as predicted by MHD simulations (Kurosawa & Romanova 2013). It was also shown that the star-disk systems can alternate between stable and unstable accretion states in timescales of just a few years (Sousa et al. 2015).

Acknowledgements. C.M. acknowledges J. Devor and T. Mazeh for making available the unofficial Corot binary catalog. S.H.P.A acknowledges financial support from CNPq, CAPES and Fapemig.

References

Affer, L., Micela, G., Favata, F., & Flaccomio, E. 2012, MNRAS, 424, 11
Affer, L., Micela, G., Favata, F., Flaccomio, E., & Bouvier, J. 2013, MNRAS, 430, 1433
Aigrain, S., Favata, F., & Gilmore, G. 2004, A&A, 414, 1139
Alencar, S. H. P., Teixeira, P. S., Guimarães, M. M., et al. 2010, A&A, 519, A88
Atwood-Stone, C., Miller, B. P., Richards, M. T., Budaj, J., & Peters, G. J. 2012, ApJ, 760, 134
Baraffe, I., Chabrier, G., Allard, F., & Hauschildt, P. H. 1998, A&A, 337, 403
Bloemen, S., Marsh, T. R., Østensen, R. H., et al. 2011, MNRAS, 410, 1787

Bouvier, J., Chelli, A., Allain, S., et al. 1999, A&A, 349, 619
Bouvier, J., Grankin, K. N., Alencar, S. H. P., et al. 2003, A&A, 409, 169
Bouvier, J., Alencar, S. H. P., Boutelier, T., et al. 2007a, A&A, 463, 1017
Bouvier, J., Alencar, S. H. P., Harries, T. J., Johns-Krull, C. M., & Romanova, M. M. 2007b, Protostars and Planets V, 479
Chapellier, E., & Mathias, P. 2013, A&A, 556, A87
Chaplin, W. J., Bedding, T. R., Bonanno, A., et al. 2011, ApJ, 732, L5
Cieza, L., & Baliber, N. 2007, ApJ, 671, 605
Cody, A. M., Stauffer, J., Baglin, A., et al. 2014, AJ, 147, 82
Collier Cameron, A., & Campbell, C. G. 1993, A&A, 274, 309
da Silva, R., Maceroni, C., Gandolfi, D., Lehmann, H., & Hatzes, A. P. 2014, A&A, 565, 55
Dahm, S. E. 2008, The Young Cluster and Star Forming Region NGC 2264, ed. B. Reipurth, 966
De Medeiros, J. R., Ferreira Lopes, C. E., Leão, I. C., et al. 2013, A&A, 555, A63
Degroote, P., Aerts, C., Baglin, A., et al. 2010, Nature, 464, 259
Degroote, P., Aerts, C., Michel, E., et al. 2012, A&A, 542, A88
Derekas, A., Kiss, L. L., Borkovits, T., et al. 2011, Science, 332, 216
Desmet, M., Frémat, Y., Baudin, F., et al. 2010, MNRAS, 401, 418
do Nascimento, J.-D., da Costa, J. S., & Castro, M. 2012, A&A, 548, L1
do Nascimento, Jr., J.-D., Takeda, Y., Meléndez, J., et al. 2013, ApJ, 771, L31
Dolez, N., Vauclair, S., Michel, E., et al. 2009, A&A, 506, 159
Fabrycky, D., & Tremaine, S. 2007, ApJ, 669, 1298
Flaccomio, E., Micela, G., Favata, F., & Alencar, S. P. H. 2010, A&A, 516, L8
Fonseca, N. N. J., Alencar, S. H. P., Bouvier, J., Favata, F., & Flaccomio, E. 2014, A&A, 567, A39
Gallet, F., & Bouvier, J. 2015, A&A, 577, A98
García, R. A., Mathur, S., Salabert, D., et al. 2010, Science, 329, 1032
Gillen, E., Aigrain, S., McQuillan, A., et al. 2014, A&A, 562, A50
Girardi, L., Groenewegen, M. A. T., Hatziminaoglou, E., & da Costa, L. 2005, A&A, 436, 895
Hambleton, K., Degroote, P., Conroy, K., et al. 2013, in EAS PS, 64, eds. K. Pavlovski, A. Tkachenko, & G. Torres, 285
Hareter, M., Paparó, M., Weiss, W., et al. 2014, A&A, 567, A124
Hartmann, L. 2002, ApJ, 566, L29
Harvey, J. 1985, in Future Missions in Solar, Heliospheric & Space Plasma Physics, eds. E. Rolfe, & B. Battrick, ESA SP, 235, 199
Huat, A.-L., Hubert, A.-M., Baudin, F., et al. 2009, A&A, 506, 95
Huber, K. F., Czesla, S., Wolter, U., & Schmitt, J. H. M. M. 2010, A&A, 514, A39
Ibanoğlu, C., Taş, G., Sipahi, E., & Evren, S. 2007, MNRAS, 376, 573
Johns-Krull, C. M., Valenti, J. A., Piskunov, N. E., Saar, S. H., & Hatzes, A. P. 2001, in Magnetic Fields Across the Hertzsprung-Russell Diagram, eds. G. Mathys, S. K. Solanki, & D. T. Wickramasinghe, ASP Conf. Ser., 248, 527
Koenigl, A. 1991, ApJ, 370, L39
Kozai, Y. 1962, AJ, 67, 591
Kulkarni, A. K., & Romanova, M. M. 2008, MNRAS, 386, 673
Kumar, P., Ao, C. O., & Quataert, E. J. 1995, ApJ, 449, 294
Kurosawa, R., & Romanova, M. M. 2013, MNRAS, 431, 2673
Lamm, M. H., Mundt, R., Bailer-Jones, C. A. L., & Herbst, W. 2005, A&A, 430, 1005
Lanza, A. F. 2008, A&A, 487, 1163
Lanza, A. F., Aigrain, S., Messina, S., et al. 2009a, A&A, 506, 255
Lanza, A. F., Pagano, I., Leto, G., et al. 2009b, A&A, 493, 193
Lanza, A. F., Bonomo, A. S., Moutou, C., et al. 2010, A&A, 520, A53
Lanza, A. F., Bonomo, A. S., Pagano, I., et al. 2011, A&A, 525, A14
Leão, I. C., Pasquini, L., Ferreira Lopes, C. E., et al. 2015, A&A, 582, A85
Lou, Y.-Q. 2000, ApJ, 540, 1102
Ludwig, H.-G., Samadi, R., Steffen, M., et al. 2009, A&A, 506, 167
Maceroni, C., & Rucinski, S. M. 1999, AJ, 118, 1819
Maceroni, C., Montalbán, J., Michel, E., et al. 2009, A&A, 508, 1375
Maceroni, C., Montalbán, J., Gandolfi, D., Pavlovski, K., & Rainer, M. 2013, A&A, 552, A60
Mathur, S., García, R. A., Morgenthaler, A., et al. 2013, A&A, 550, A32
McGinnis, P. T., Alencar, S. H. P., Guimarães, M. M., et al. 2015, A&A, 577, A11
Ménard, F., & Bertout, C. 1999, in NATO Advanced Science Institutes (ASI) Series C, 540, eds. C. J. Lada, & N. D. Kylafis, 341
Michel, E., Samadi, R., Baudin, F., et al. 2009, A&A, 495, 979
Miglio, A., Chiappini, C., Morel, T., et al. 2013, in Eur. Phys. J. Web Conf., 43, 3004
Mimica, P., & Pavlovski, K. 2012, in IAU Symp. 282, eds. M. T. Richards, & I. Hubeny, 63
Mosser, B., Baudin, F., Lanza, A. F., et al. 2009a, A&A, 506, 245
Mosser, B., Michel, E., Appourchaux, T., et al. 2009b, A&A, 506, 33
Oliver, R., Ballester, J. L., & Baudin, F. 1998, Nature, 394, 552
Popper, D. M., & Etzel, P. B. 1981, AJ, 86, 102
Rieger, E., Kanbach, G., Reppin, C., et al. 1984, Nature, 312, 623
Salabert, D., Régulo, C., Ballot, J., García, R. A., & Mathur, S. 2011, A&A, 530, A127
Samadi, R., Belkacem, K., Ludwig, H.-G., et al. 2013, A&A, 559, A40
Sarro, L. M., Debosscher, J., Neiner, C., et al. 2013, A&A, 550, A120
Schlafly, E. F., & Finkbeiner, D. P. 2011, ApJ, 737, 103
Shu, F., Najita, J., Ostriker, E., et al. 1994, ApJ, 429, 781

Silva-Valio, A., & Lanza, A. F. 2011, A&A, 529, A36
Silva-Valio, A., Lanza, A. F., Alonso, R., & Barge, P. 2010, A&A, 510, A25
Sokolovsky, K., Maceroni, C., Hareter, M., et al. 2010, Communications in Asteroseismology, 161, 55
Sousa, A., Alencar, S., Bouvier, J., et al. 2015, ArXiv e-prints
Southworth, J., Maxted, P. F. L., & Smalley, B. 2004, MNRAS, 351, 1277
Stauffer, J., Cody, A. M., Baglin, A., et al. 2014, AJ, 147, 83
Stauffer, J., Cody, A. M., McGinnis, P., et al. 2015, AJ, 149, 130
Tal-Or, L., Santerne, A., Mazeh, T., et al. 2011, A&A, 534, A67
Tal-Or, L., Mazeh, T., Alonso, R., et al. 2013, A&A, 553, A30
Tal-Or, L., Faigler, S., & Mazeh, T. 2015, A&A, 580, A21
van't Veer, F., & Maceroni, C. 1989, A&A, 220, 128
Vilhu, O. 1982, A&A, 109, 17
Welsh, W. F., Orosz, J. A., Aerts, C., et al. 2011, The ApJS, 197, 4
Zucker, S., Mazeh, T., & Alexander, T. 2007, ApJ, 670, 1326
Zwintz, K., Fossati, L., Ryabchikova, T., et al. 2013, A&A, 550, A121

Acknowledgements: The CoRoT space mission has been developed and operated by CNES, with the contribution of Austria, Belgium, Brazil, ESA, Germany, and Spain.